

Accelerating Iterative Linear Equation Solver Using Modified Domain-Wall Fermion Matrix in Lattice QCD Simulations

Wei-Lun Chen[1(✉)], Issaku Kanamori[2], Hideo Matsufuru[3], and Hartmut Neff[4]

[1] Particle and Nuclear Physics, Graduate Institute for Advanced Studies, Graduate University for Advanced Studies (SOKENDAI), Oho 1-1, Tsukuba 305-0801, Japan
wlchen@post.kek.jp

[2] RIKEN Center for Computational Science, 7-1-26 Minatojima-minami-machi, Chuo-ku, Kobe, Hyogo 650-0047, Japan
kanamori-i@riken.jp

[3] Computing Research Center, High Energy Accelerator Research Organization (KEK), Accelerator Science Program, Graduate University for Advanced Studies (SOKENDAI), Oho 1-1, Tsukuba 305-0801, Japan
hideo.matsufuru@kek.jp

[4] Luzernerstrasse 43, 6330 Cham, Switzerland
hartmutneff@aol.com

Abstract. Lattice simulations of Quantum Chromodynamics (QCD) enable one to calculate low-energy properties of the strong interaction among quarks and gluons based on the first principle. The most time-consuming part of the numerical simulations of lattice QCD is typically solving a linear equation for the quark matrix. In particular, a discretized quark formulation called the domain-wall fermion operator requires a large numerical cost while retaining the lattice version of the chiral symmetry to good precision. The domain-wall operator is defined on a five-dimensional (5D) space extending the four-dimensional (4D) spacetime with an extra fifth coordinate. After solving the linear equation in 5D space, the result vector is projected onto the original 4D space. There is a variant of the domain-wall operator that improves the convergence of the 5D linear equation while unchanging the 4D solution vector. In this paper, we examine how this variant of the domain-wall operator accelerates the iterative linear equation solver in practical setups. We also measure the eigenvalues of the operator and compare the condition number with the convergence of the solver. We use a generic lattice QCD code set Bridge++ that is planned to be released including the improved form of the domain-wall operator examined in this work with code for GPU.

Keywords: lattice QCD · iterative linear equation solver · high performance computing

© The Author(s), under exclusive license to Springer Nature Switzerland AG 2026
O. Gervasi et al. (Eds.): ICCSA 2025 Workshops, LNCS 15890, pp. 54–69, 2026.
https://doi.org/10.1007/978-3-031-97606-3_5

1 Introduction

Large-scale simulations of lattice Quantum Chromodynamics (QCD) have been a challenge of the high performance computing for long time. The QCD is the fundamental theory of the strong interaction among quarks and gluons, which is formulated based on the invariance under the local SU(3) gauge transformation on the color degree of freedom of the quark and gluon fields. While the fundamental theory is known, it is quite difficult to solve it analytically because of the strong coupling of this theory. The lattice QCD is a field theory formulated on the Euclidean discretized spacetime. Employing the path integral quantization, this theory enables numerical evaluation of the physical quantities using the Monte Carlo algorithms. Thus the lattice QCD simulations provide a general procedure to investigate the QCD based on the first principle. Such calculation is particularly important in the search for phenomena beyond the Standard Model of particle physics through precision evaluation of the hadronic scattering processes. Lattice QCD is also important in the quantitative understanding of the nuclear force among hadrons, the phase structure of QCD at finite temperature and density, and so on.

The most time-consuming part of lattice QCD simulation is solving a linear equation for the quark (fermion) matrix, which is typically large and sparse, and thus solved by iterative Krylov subspace methods. There is a variety in the form of a fermion matrix since the only required condition is that it approaches QCD in the continuum limit. In this paper, we focus on the type of matrix called the domain-wall fermion operator. This fermion matrix has an important feature that preserves the chiral symmetry, an important symmetry of QCD, on the lattice with good precision. The domain-wall operator is defined in the five-dimensional (5D) space, which extends the four-dimensional (4D) spacetime by adding the fifth-coordinate. The physical modes in the original four-dimensional space are picked up from the two edges in the fifth direction. Since the domain-wall fermion matrix is defined in the 5D space, the numerical cost is higher than other formulations. Thus improving the convergence of the fermion matrix solver is a quite important subject in numerical simulations.

One of the authors (H. Neff) proposed a form of the domain-wall operator that improves the convergence of the solver while unchanging the physical modes in the 4D space [16]. This paper aims to conduct a systematic and practical investigation of Neff's form and how it improves the convergence of solvers. While Ref. [16] already examined the effect of the improved form on several parameter sets, we add several new setups including the operator with the link smearing. We determine the condition number of the matrix by measuring the lowest and highest eigenvalues of the Hermitian domain-wall matrix and compare with the convergence of the Conjugate Gradient (CG) solver. In numerical study, we employ the Bridge++ code set [1] with an extension to incorporate Neff's improved form of the domain-wall matrix. We use the code for GPU implemented with OpenACC [7].

This paper is organized as follows. The next section introduces the lattice QCD and our target fermion matrix in a certain depth. While the equations

necessary to implement the fermion matrix used in this work are displayed to make the description self-contained, the essential ingredient is the introduction of a tunable parameter α in the 5D matrix that does not change the 4D solution vector. Section 3 shows our numerical results. We examine the effect of α in the modified matrix on the convergence of the CG solver. The last section is devoted to the conclusion and outlook.

2 Lattice QCD

2.1 Lattice QCD and Chiral Symmetry

The lattice QCD action in four-dimensional Euclidean space is written as follows:

$$S_{\mathrm{QCD}} = \sum_x \left\{ (S_G[U_\mu(x)] + \bar{\psi}(x) D_F[U] \psi(x) \right\}, \tag{1}$$

where S_G is a gauge action, $\psi(x)$ and $\bar{\psi}(x)$ anti-commuting Grassmann fields representing quark and anti-quark, $D_F[U]$ a fermion operator depending on the link variable $U_\mu(x)$, $x = (x_1, x_2, x_3, x_4)$ a lattice site, where the lattice spacing a is set to unity for simplicity. $U_\mu(x)$ is a 3×3 complex matrix field representing the gauge field. ψ has the color and spinor degrees of freedom in addition to the lattice site x. The spinor has four components that represent the up and down spin for quark and anti-quark. Thus the quark field has $3 \times 4 = 12$ complex components on each site x.

Employing the path integral quantization, the QCD partition function reads

$$\begin{aligned} \int \mathcal{D}U \mathcal{D}\psi \mathcal{D}\bar{\psi} \exp\left[-S_G - \bar{\psi}(x) D_F[U] \psi(x) \right] &= \int \mathcal{D}U \det(D_F) e^{-S_G} \\ &= \int \mathcal{D}U \mathcal{D}\phi \mathcal{D}\phi^\dagger \exp\left[-S_G - \frac{1}{2} \phi^\dagger(x) D_F[U]^{-1} \phi(x) \right], \end{aligned} \tag{2}$$

where complex (ordinary number) field $\phi(x)$ is introduced as Gaussian integration variables. Applying a Monte Carlo method, an expectation value of physical observable $\mathcal{O}$ is represented as

$$\langle \mathcal{O}[U, \psi, \bar{\psi}] \rangle = \frac{1}{N} \sum_i^N O[U^{(i)}, S_q^{(i)}]. \tag{3}$$

Here, the gauge field configurations $\{U^{(i)}\}$ are assumed to be generated with the Boltzmann weight $\exp[-S_G] \det(D_F)$, and $S_q^{(i)}$ is a quark propagator obtained by solving a linear equation for the fermion matrix D_F,

$$D_F[U^{(i)}]_{y,x} S_q^{(i)}(x) = b_y, \tag{4}$$

where the color and spinor indices are omitted for simplicity. To obtain the physical quantities with high precision, one needs to solve this linear equation many times to calculate $O[U^{(i)}, S_q^{(i)}]$. Furthermore, the linear equation solver is

called many times during the Monte Carlo generation of the gauge configurations. Thus solving this linear equation is a typical bottleneck of lattice QCD simulations.

In discretizing the continuum QCD action, there is a variation of the action on the lattice, since the only required condition is that the lattice action approaches to the QCD action in the continuum limit, $a \to 0$, where a is the lattice spacing. Thus there has been proposed a number of lattice actions intending rapid approach to the continuum limit. Each lattice fermion action has its pros and cons. One of the most popular fermion operators is the Wilson fermion,

$$D_W(x,y;M) = (4+M)\delta_{x,y} - \frac{1}{2}\sum_{\mu=1}^{4}\Big\{(1-\gamma_\mu)U_\mu(x)\delta_{x+\hat{\mu},y} + (1+\gamma_\mu)U_\mu^\dagger(x-\hat{\mu})\delta_{x-\hat{\mu},y}\Big\}, \quad (5)$$

where M is quark mass, $\hat{\mu}$ is a unit vector in μ-th direction ($\mu = 1,2,3,4$), γ_μ is a 4×4 complex matrix acting on the spinor components. The improved form of the Wilson fermion action called clover fermion is extensively used in large-scale simulations of lattice QCD. It has a disadvantage, however, that a symmetry called chiral symmetry, which is satisfied by the QCD action for vanishing quark mass, is explicitly violated even with setting $M = 0$.

In the continuum QCD, the chiral symmetry is represented as

$$\gamma_5 D_F + D_F \gamma_5 = 0, \quad (6)$$

where $\gamma_5 = \gamma_1\gamma_2\gamma_3\gamma_4$. This symmetry concerns the left- and right-handed components of the quark field. The spontaneous break-down of this symmetry at low-energy ensures the smallness of the pion masses and is attributed to the most of the masses of proton and neutron. The chiral symmetry is also the basis of the phenomenological properties of the hadrons, as typically represented by the soft pion theorem that declares that the coupling between a hadron and a pion vanishes as the transferred energy becomes small. Thus the quark action that respects the chiral symmetry is particularly important in understanding the chiral dynamics of QCD. For the Wilson fermion action, the chiral symmetry is restored only in the continuum limit.

On the lattice, the chiral symmetry had been a difficulty for a long time. Understanding of the chiral symmetry on the lattice was proceeded by the discovery that the exact chiral symmetry on the lattice is represented by the Ginsparg-Wilson relation [11],

$$\gamma_5 D_F + D_F \gamma_5 = a D_F R \gamma_5 D_F, \quad (7)$$

where R is a certain constant [12,14]. Thereafter several fermion actions that satisfies the Ginsparg-Wilson relation exactly or approximately have been proposed. The Domain-wall fermion is the latter kind of formulation and in the limit of the infinite extent of the fifth direction, $L_s \to \infty$, it satisfies the Ginsparg-Wilson relation exactly.

2.2 Domain-Wall Fermion Matrix

The domain-wall fermion was proposed by Kaplan [13] intending to formulate the chiral gauge theory. The domain-wall fermion is defined on the five-dimensional space by adding the fifth coordinate, $s = 1, \ldots, L_s$, to the four-dimensional spacetime and by introducing a large negative mass to the Wilson operator kernel (5). The light modes appear in the two edges of the fifth direction. After the realization of the domain-wall fermion as a light fermion formulation [10,17], several improved forms have been proposed [3,6,8]. These variants are described by the following form [6]:

$$D_{DW} = \begin{pmatrix} D_+^{(1)} & D_-^{(1)}P_- & 0 & \cdots & 0 & -mD_-^{(1)}P_+ \\ D_-^{(2)}P_+ & D_+^{(2)} & D_-^{(2)}P_- & & & 0 \\ 0 & D_-^{(3)}P_+ & D_+^{(3)} & D_-^{(3)}P_- & & 0 \\ \vdots & & \ddots & \ddots & \ddots & \vdots \\ 0 & & & D_-^{(L_s-1)}P_+ & D_+^{(L_s-1)} & D_-^{(L_s-1)}P_- \\ -mD_-^{(L_s)}P_- & 0 & \cdots & 0 & D_-^{(L_s)}P_+ & D_+^{(L_s)} \end{pmatrix}, \quad (8)$$

where m is the quark mass, $P_- = (1-\gamma_5)/2$, $P_+ = (1+\gamma_5)/2$,

$$D_+^{(s)} = b_s D_W + 1, \qquad D_-^{(s)} = c_s D_W - 1, \quad (9)$$

$D_W = D_W(-M_0)$ is the Wilson operator (5) with large negative mass $-M_0$, where $M_0 = O(1)$ is called the domain-wall height. There are several choices for the parameters b_s and c_s: $(b_s, c_s) = (1, 0)$ [10,17], $(b_s, c_s) = (1, 1)$ [3], $b_s - c_s =$ const. (independent of s) called the Möbius fermion [6], and $b_s = c_s$ chosen depending on s so as to optimize the Ginsparg-Wilson relation [8]. In this paper we only examine the cases $(b_s, c_s) = (b, c)$ independent of s.

In the fifth direction, the following boundary condition is imposed at $s = 1$ and L_s:

$$P_+\psi(s=0) = P_-\psi(s=L_s+1) = 0. \quad (10)$$

The fermion field in four-dimensional space is given as[1]

$$\begin{aligned} q(x) &= P_-\,\psi(x, s{=}1) + P_+\,\psi(x, s{=}L_s), \\ \bar{q}(x) &= \bar{\psi}(x, s{=}1)(-D_-^{(1)})P_+ + \bar{\psi}(x, s{=}L_s)(-D_-^{(L_s)})P_-. \end{aligned} \quad (11)$$

In the limit of $L_s \to \infty$, the lattice chiral symmetry is satisfied exactly. This limit corresponds to the overlap fermion operator, $D_{\rm ov} = \mathrm{sign}(\gamma_5 D_W)$, which practically requires large numerical resources.

Link Smearing. Recently link smearing is frequently adopted as an improvement procedure for fermion actions. The link smearing is essentially the integration of the surrounding gauge field into the link variable, $U_\mu(x)$. We consider the stout projection combined with the APE smearing [15]:

$$C_\mu(x) = \sum_{\nu\neq\mu} \rho \left[U_\nu(x) U_\mu(x{+}\hat{\nu}) U_\nu^\dagger(x{+}\hat{\mu}) + U_\nu^\dagger(x{-}\hat{\nu}) U_\mu(x{-}\hat{\nu}) U_\nu(x{-}\hat{\nu}{+}\hat{\mu}) \right],$$

[1] This definition of $\bar{q}(x)$ corresponds to $\tilde{q}_x$ called "traditional choice" in Ref. [5].

$$U_\mu(x)' = \exp\left([C_\mu(x)U_\mu^\dagger(x)]_{\mathrm{AT}}\right) U_\mu(x), \tag{12}$$

where $[\cdots]_{\mathrm{AT}}$ represents anti-Hermitian and traceless operation, and ρ is a tunable parameter. This smearing step (12) can be repeatedly applied. The fermion operator can be improved by adopting the smeared link variable instead of the original one.

2.3 Better Conditioned Form of Domain-Wall Operator

An improved form of the domain-wall fermion operator which unchanges the four-dimensional fermion field was proposed by H. Neff [16]. This form is represented as follows.

$$D_{DW}^{(\alpha)} = \begin{pmatrix} D_+^{(1)}(P_- + \alpha P_+) & \alpha D_-^{(1)} P_- & 0 & \cdots & -mD_-^{(1)}P_+ \\ \alpha D_-^{(2)} P_+ & \alpha D_+^{(2)} & \alpha D_-^{(2)} P_- & & 0 \\ \vdots & \ddots & \ddots & \ddots & \vdots \\ -mD_-^{(N)} P_- & 0 & \cdots & \alpha D_-^{(N)} P_+ & D_+^{(N)}(P_+ + \alpha P_-) \end{pmatrix} \tag{13}$$

Note that except for the four corners of the fifth coordinate matrix, each four-dimensional block is multiplied by α. The top-left and bottom-right blocks are modified by multiplied by $(P_\mp + \alpha P_\pm)$, respectively, and top-right and bottom-left blocks are unchanged. This modification does not change the four-dimensional quark field, while affecting the convergence of the linear equation in five-dimensional space.

There is a relation between $D_{DW}^{(\alpha)}$ and $D_{DW} = D_{DW}^{(\alpha=1)}$ that

$$D_{DW}^{(\alpha)} \mathcal{P} = D_{DW}^{(\alpha=1)} \mathcal{P}\mathcal{A}, \tag{14}$$

where

$$\mathcal{P} = \begin{pmatrix} P_- & P_+ & 0 & \cdots & 0 \\ 0 & P_- & P_+ & \ddots & \vdots \\ \vdots & \ddots & \ddots & \ddots & 0 \\ 0 & & \ddots & P_- & P_+ \\ P_+ & 0 & \cdots & 0 & P_- \end{pmatrix}, \qquad \mathcal{A} = \begin{pmatrix} 1 & 0 & & \cdots & 0 \\ 0 & \alpha & 0 & & \vdots \\ \vdots & \ddots & \ddots & \ddots & \vdots \\ \vdots & & \ddots & \alpha & 0 \\ 0 & \cdots & \cdots & 0 & \alpha \end{pmatrix}. \tag{15}$$

We need to solve a 5D equation

$$D_{DW}^{(\alpha=1)} x_5 = b_5, \tag{16}$$

where according to Eq. (11), $b_5 = (-D_-)\mathcal{P}^\dagger(0, \cdots, 0, b_4)^T$ for a 4D source vector b_4 with $D_- = \mathrm{diag}(D_-^{(1)}, \cdots, D_-^{(L_s)})$. Once a 5D solution vector x_5 is determined, the 4D solution vector x_4 is provided as $x_4 = [\mathcal{P}^\dagger x_5]_{s=1}$. Due to the relation (14), the solution of $D_{DW}^{(\alpha)} x_5^{(\alpha)} = b_5$ gives the same 4D solution x_4, since

$$\mathcal{P}^\dagger x_5 = (D_{DW}\mathcal{P})^{-1} b_5 = (D_{DW}^{(\alpha)}\mathcal{P}\mathcal{A}^{-1})^{-1} b_5 = \mathcal{A}\mathcal{P}^\dagger (D_{DW}^{(\alpha)})^{-1} b_5 = \mathcal{A}\mathcal{P}^\dagger x_5^{(\alpha)}, \tag{17}$$

where $\mathcal{P}^\dagger = \mathcal{P}^{-1}$, and $[\mathcal{A}\mathcal{P}^\dagger x_5^{(\alpha)}]_{s=1} = [\mathcal{P}^\dagger x_5^{(\alpha)}]_{s=1}$. Thus if the linear equation with $\alpha \neq 1$ can be solved faster than the original equation (16), the numerical cost would be reduced.

Even-Odd Preconditioning. Noting that the D_W and D_{DW} contain nearest neighbor coupling, by dividing sites into even and odd sites, $D_{DW}x = b$ is represented as

$$D_{DW}\, x = \begin{pmatrix} D_{ee} & D_{eo} \\ D_{oe} & D_{oo} \end{pmatrix} \begin{pmatrix} x_e \\ x_o \end{pmatrix} = \begin{pmatrix} b_e \\ b_o \end{pmatrix} = b. \tag{18}$$

One arrives at the even-odd preconditioned linear equation,

$$D\, x_e \equiv (1 - D_{ee}^{-1} D_{eo} D_{oo}^{-1} D_{oe})\, x_e = \tilde{b}_e, \tag{19}$$

$$\tilde{b}_e = D_{ee}^{-1}(b_e - D_{eo} D_{oo}^{-1} b_o), \tag{20}$$

$$x_o = D_{oo}^{-1}(b_o - D_{oe} x_e). \tag{21}$$

One needs to solve Eq. (19) whose matrix D usually has a smaller condition number than D_{DW}. There are two ways to divide the sites into even and odd: In the five-dimension space, or four-dimensional space. We adopt the latter for simplicity and similarity with other fermion formulations. Since this paper focuses on the effect of α on the convergence of iterative solver, we do not concern the details of implementation and its performance, which is described in [7].

Note that there is another version of even-odd preconditioned equation,

$$(1 - D_{eo} D_{oo}^{-1} D_{oe} D_{ee}^{-1})\, y_e = b'_e, \tag{22}$$

where $b'_e = b_e - D_{eo} D_{oo}^{-1} b_o$ and $x_e = D_{ee}^{-1} y_e$. However, the relation (14) means $D_{DW}^{(\alpha)} = D_{DW}(\mathcal{P}\mathcal{A}^{-1}\mathcal{P}^\dagger)$, and thus $D_{ee}^{(\alpha)} = D_{ee}^{(\alpha=1)}(\mathcal{P}\mathcal{A}^{-1}\mathcal{P}^\dagger)$ and so on. In Eq. (22), $(\mathcal{P}\mathcal{A}^{-1}\mathcal{P}^\dagger)$ and $(\mathcal{P}\mathcal{A}^{-1}\mathcal{P}^\dagger)^{-1} = \mathcal{P}\mathcal{A}\mathcal{P}^\dagger$ cancel each other, which results in no effect on the convergence of solver.

In lattice QCD simulations, the BiCGStab algorithm works in many cases as a good choice. However, for the domain-wall fermion matrix, the BiCGStab does not converge in general. This is because the eigenvalues of D_{DW} distribute in the region of negative real part. Thus the CG algorithm for $D^\dagger D$ is applied, where "†" denotes Hermitian conjugate, *i.e.*, taking complex conjugate and transpose of the matrix D in Eq. (19).

It is well-known that a single precision solver can work as a preconditioner in the solver in the double precision which is the precision practically required in numerical simulations. In such a multi-precision solver, most of the time is consumed in the single precision solver and hence the performance of matrix multiplication to a vector in single precision determines the efficiency of solver algorithms. It is also expected that the convergence property of the iterative solver is not much different for double and single precision. Thus in the following we show the solver convergence for the single precision solver only.

3 Results

3.1 Numerical Setup

We perform a numerical experiment to investigate how the introduction of the parameter α improves the convergence of five-dimensional solver. For practical

investigation, we generate three ensembles of gauge configuration generated with quenched approximation, namely without the quark vacuum polarization effect. They are generated with the plaquette gauge action at the gauge coupling $\beta = 6.0$ and 5.7, which roughly correspond to the values of lattice spacing $a \simeq 0.1$ and 0.2 fm, respectively. For $\beta = 6.0$, two lattice volumes 16^4 and 32^4 are adopted. For the $\beta = 5.7$, we generate a 16^4 lattice that roughly corresponds to the same physical volume as the 32^4 lattice with $\beta = 6.0$. On these configurations, the parameter of the domain-wall operator $M_0 = 1.8$ is used as a typical value in practical simulations, as adopted by the RBC/UKQCD Collaboration [2].

To examine the effect of the link smearing, we apply three steps of the stout projection [15] with the APE smearing with $\rho = 0.1$. This setup corresponds to that adopted by the JLQCD collaboration [9]. In this case $M_0 = 1.0$ is adopted since the lattice artifact to shift the best value of M_0 from 1 due to the interaction is largely suppressed.

On these ensembles, the parameters $(b, c) = (1.5, 0.5)$ and $(1.0, 1.0)$ are adopted with two values of $L_s = 8$ and 16. The values of parameters $(b, c) = (1.5, 0.5)$ are adopted by JLQCD Collaboration [9] and RBC/UKQCD Collaboration [2], and $(b, c) = (1.0, 1.0)$ corresponds to the Borici's form [3]. We observe the convergence of the CG solver for several values of quark mass in the range of m =0.001–0.01, with varying the value of α.

As the simulation code, we employ the Bridge++ code set [1,4] with an extension to offloading code for GPU implemented using OpenACC [7]. The numerical computation is performed on the Pegasus system at University of Tsukuba, whose each node is composed of one Intel Xeon processor and one NVIDIA H100 GPU. All the computation is performed on a single process with a single GPU device. Since this work concerns the algorithmic convergence of an iterative solver, we do not discuss the performance of the code which is described in [7].

3.2 Result for $\beta = 6.0$ on the 16^4 Lattice

Let us start with examining the effect of α on the convergence of CG solver on the 16^4 lattice generated with the gauge coupling $\beta = 6.0$. In the unsmeared cases, we set $M_0 = 1.8$ as aforementioned. The CGNR solver is applied in the single precision with the convergence criterion $|r|^2 < 10^{-14}$.

Figure 1 shows the converged iteration number against α on a single configuration without the link smearing. Fluctuation against the gauge configuration will be discussed later. The top panels of Fig. 1 display the result for $(b, c) = (1.5, 0.5)$ with $L_s = 8$ and 16. For $L_s = 8$, setting $\alpha \simeq 0.6$ gives the best-improved result and reduces the interation counts by 25% compared to the $\alpha = 1$ case independently of the quark mass. While $L_s = 16$ requires slightly more iterations until convergence, the result shows the same tendency that $\alpha \simeq 0.6$ is the best, while the amount of improvement decreases as the quark mass becomes larger, from 25% for $m = 0.001$ to 20% for $m = 0.01$.

The bottom panels of Fig. 1 display the result for $(b, c) = (1.0, 1.0)$ (Borici's setting). For the both of $L_s = 8$ and 16 cases, $\alpha \simeq 0.5$ improves the conver-

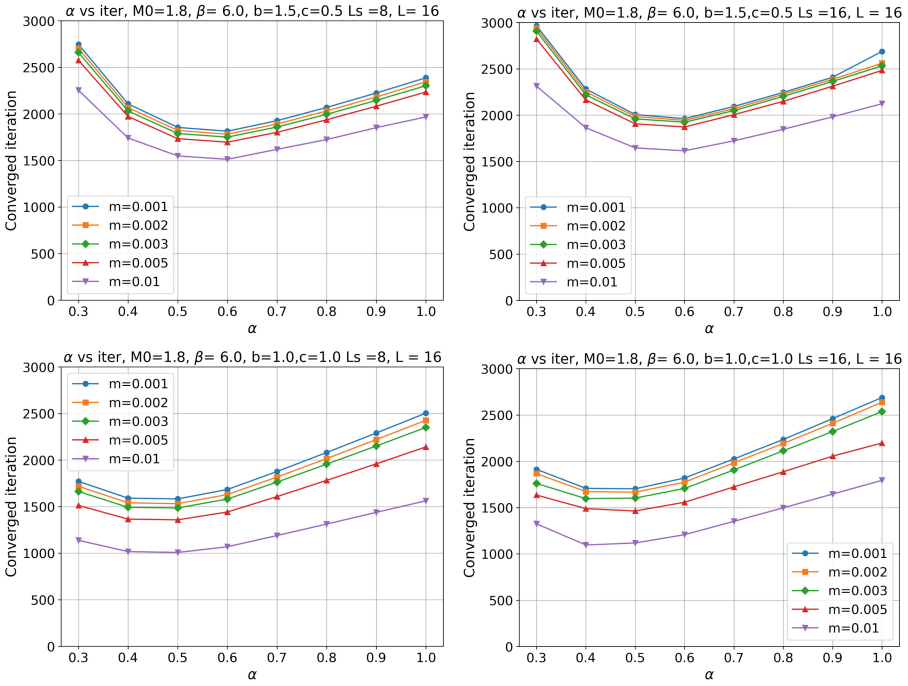

Fig. 1. Converged number of CG iteration for $\beta = 6.0$ on $(L = 16)^4$ lattice, $M_0 = 1.8$ (without smearing), $(b, c) = (1.5, 0.5)$ (top panels) $L_s = 8$ (left) and 16 (right) and $(b, c) = (1.0, 1.0)$ (bottom panels).

gence most, for which about 36% acceleration is achieved independently of the quark mass and L_s. As an observation, the quark mass dependence of converged iteration is larger than the case of $(b, c) = (1.5, 0.5)$.

Next we observe the effect of the link smearing. For the domain-wall operator with the smeared link, we set $M_0 = 1.0$. The top panels of Fig. 2 show the result for $(b, c) = (1.5, 0.5)$. Together with the link smearing, this choice of the parameters corresponds to the setup adopted by JLQCD Collaboration, except for the configuration in this work is in the quenched approximation. Around $\alpha \simeq 0.5$, the converged number of CG iteration becomes minimum where 37% acceleration is achieved for $m = 0.001$. We find that changing L_s does not affect the optimal value of α, and has only little effect on the iteration number for the convergence.

The bottom panels of Fig. 2 shows the result for $(b, c) = (1.0, 1.0)$. A similar tendency to the $(b, c) = (1.5, 0.5)$ case is found while the best value of α becomes around 0.4. The achieved speed-up is about 40 % for $m = 0.001$. Also a small effect of L_s on the convergence is observed.

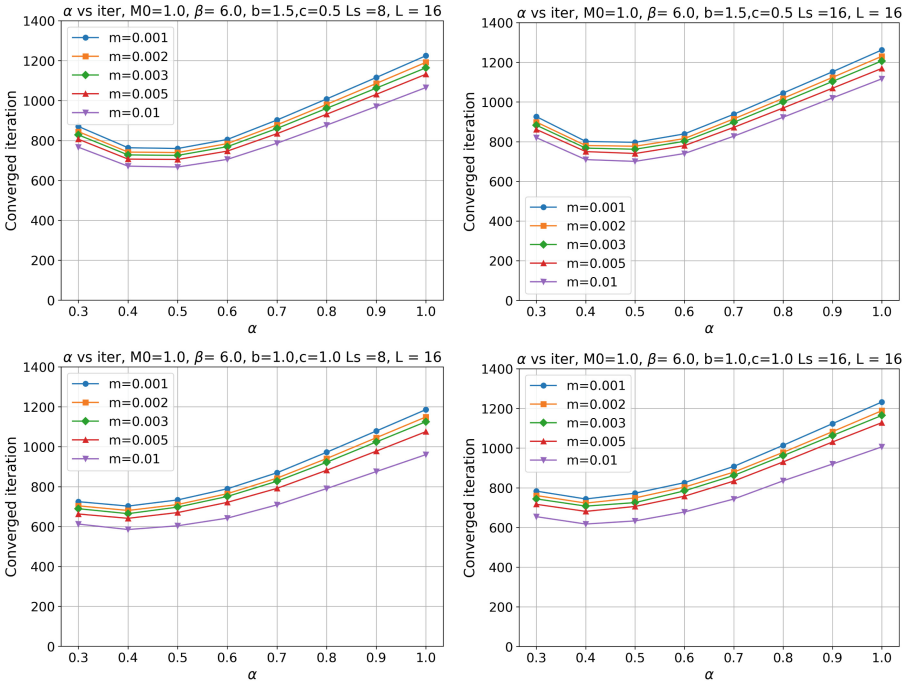

Fig. 2. Converged number of CG iteration for $\beta = 6.0$ on $(L = 16)^4$ lattice, $M_0 = 1.0$ (with smearing), $(b, c) = (1.5, 0.5)$ (top panels) $L_s = 8$ (left) and 16 (right) and $(b, c) = (1.0, 1.0)$ (bottom panels).

Condition Number. The convergence of the CG algorithm is represented by the condition number which is defined as the ratio of the maximum and minimum eigenvalues of the matrix. We measure the minimum and maximum eigenvalues of $D^\dagger D$ by applying the implicitly restarted Lanczos algorithm in the double precision, which is implemented in the Bridge++ code.

In Fig. 3, the measured condition number against the value of α is displayed for the domain-wall operators $D^\dagger D$ without the link smearing. We display the result for $(b, c) = (1.5, 0.5)$ (top panels) and $(b, c) = (1.0, 1.0)$ (bottom) for $m = 0.001$. The left panels show the values of the computed condition number on three configurations. While the fluctuation of the condition number against configuration is substantial, as displayed in the right panels of Fig. 3, normalizing by the values at $\alpha = 1$, the effect of α itself is stable. The α dependence of the condition number exhibits similar behavior as the converged number of iteration shown in Fig. 1, which is consistent with the theoretical expectation.

Figure 4 shows the condition numbers and those normalized by the values at $\alpha = 1.0$ for $D^\dagger D$ with the link smearing. Similarly to the case without smearing, the behavior of the condition numbers is consistent with the converged num-

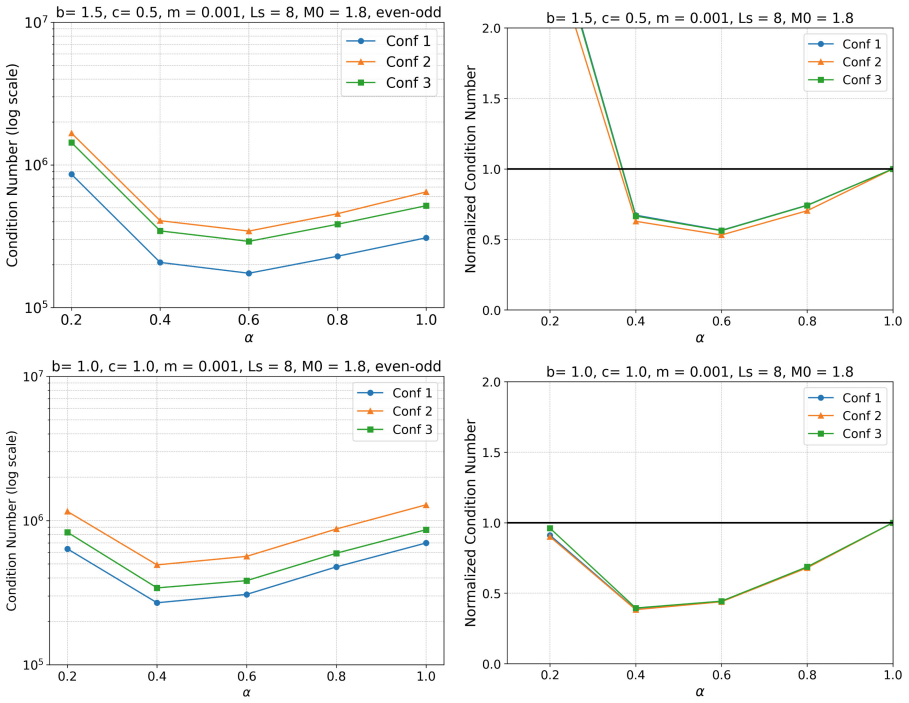

Fig. 3. The result of the condition number on the 16^4 lattice at $\beta = 6.0$ for the domain-wall operator without link smearing with parameters $M_0 = 1.8$, $(b, c) = (1.5, 0.5)$ (top panels) and $(1.0, 1.0)$ (bottom), $m = 0.001$. The left panels show the observed condition number on three configurations. The right panels show the condition numbers normalized by the values for $\alpha = 1$.

ber of CG iterations in Fig. 4. It is also observed that the fluctuation against configuration is absorbed by normalizing with the values at $\alpha = 1$.

3.3 Result for $\beta = 6.0$ on the 32^4 Lattice

To examine the effect of lattice volume on the convergence of the CG algorithm, we measure the converged iteration number against α on a 32^4 lattice with configurations generated at the gauge coupling $\beta = 6.0$. This means that the lattice volume is doubled in each direction compared to the lattice examined in the previous subsection. On this lattice size, we only show the results for $L_s = 8$.

Figure 5 shows the results of the converged number of CG iteration for unsmeared and smeared cases with $(b, c) = (1.5, 0.5)$ and $(1.0, 1.0)$. The acceleration of CG convergence for $m = 0.001$, the severest one of the measured quark masses, is in the range of 22% (top-left panel)–39% (bottom panels).

As a different feature from the results on 16^4 lattice in Figs 1 and 2, large dependence on the quark mass is observed. This is considered that the 16^4 lattice

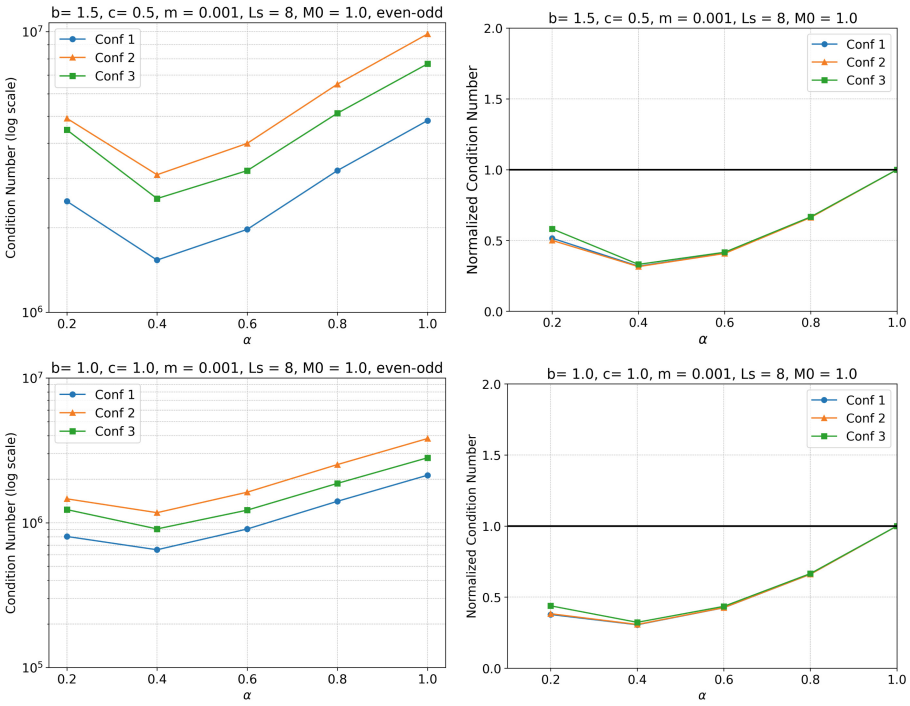

Fig. 4. The result of the condition number on the 16^4 lattice at $\beta = 6.0$ for the domain-wall operator with link smearing with parameters $M_0 = 1.0$, $(b, c) = (1.5, 0.5)$ (top panels) and $(1.0, 1.0)$ (bottom), $m = 0.001$. The left panels show the observed condition number on three configurations. The right panels show the condition numbers normalized by the values for $\alpha = 1$.

may be affected by finite volume effect, since for the present small values of quark mass, the lattice size of about 1.6 fm is not sufficiently larger than the pion Compton wavelength. This should be examined by observing the pion spectrum by varying the lattice volume.

In the context of this paper, we focus on the effect of α on the convergence number of iterations. As Fig. 5 shows, the optimal values of α are almost unchanged from those on the 16^4 lattice at the same β with similar improving rates. This result implies that incorporating α in the domain-wall operator results in improved convergence of the even-odd preconditioned CG solver almost independently of lattice volume.

3.4 Result for $\beta = 5.7$ on the 16^4 Lattice

We also examine a 16^4 lattice with configurations generated at $\beta = 5.7$, which roughly corresponds to the lattice spacing $a \simeq 0.2$ fm. This implies that the physical volume is almost the same as that of 32^4 lattice at $\beta = 6.0$. We adopt

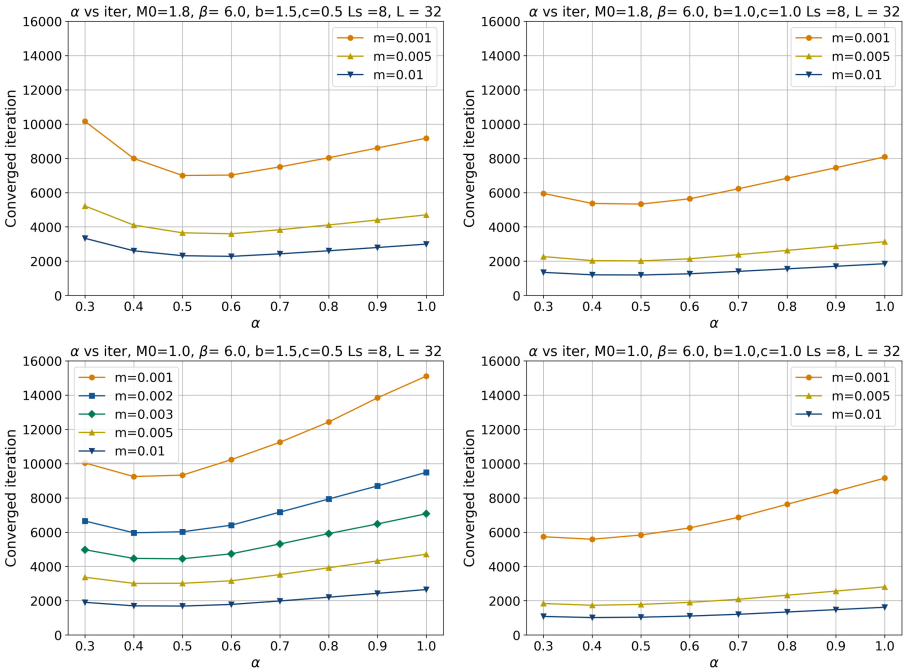

Fig. 5. Converged numbers of CG iteration on 32^4 lattice at $\beta = 6.0$. Top panels show $M_0 = 1.8$ (without smearing), $(b, c) = (1.5, 0.5)$ (left) and $(b, c) = (1.0, 1.0)$ (right). The bottom panels show $M_0 = 1.0$ (with smearing), $(b, c) = (1.5, 0.5)$ (left) and $(b, c) = (1.0, 1.0)$ (right). In both cases, $L_s = 8$ is used.

the same values of the quark mass m in lattice units as those for $\beta = 6.0$, which means that the mass in physical units is halved correspondingly.

Figure 6 shows that the α improvement effect diminishes as the quark mass increases. Similar to the case of $\beta = 6.0$, the optimal improvement is observed when α is in the range of 0.4 to 0.6. The acceleration of CG convergence for $m = 0.001$ is in the range of 24% (bottom-left panel)–39% (top-right).

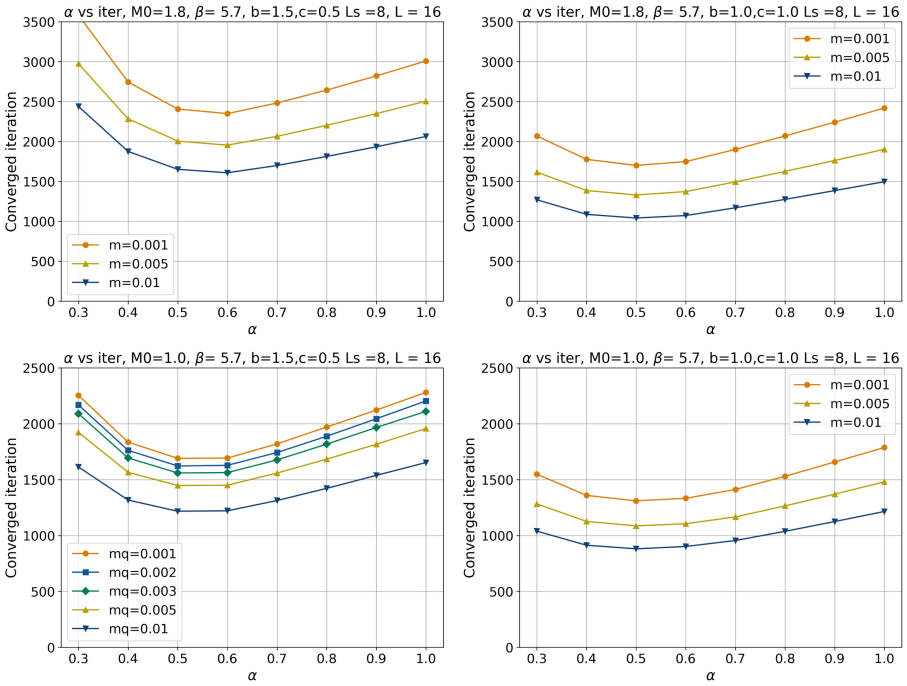

Fig. 6. Converged numbers of CG iteration on 16^4 lattice at $\beta = 5.7$. Top panels show $M_0 = 1.8$ (without smearing), $(b, c) = (1.5, 0.5)$ (left) and $(b, c) = (1.0, 1.0)$ (right). The bottom panels show $M_0 = 1.0$ (with smearing), $(b, c) = (1.5, 0.5)$ (left) and $(b, c) = (1.0, 1.0)$ (right). In both cases, $L_s = 8$ is used.

Table 1. Summary of the results. The values of α most accelerating the convergence is chosen for $m = 0.001$ and $L_s = 8$.

lattice	β	a [fm]	Smearing	M_0	(b, c)	Best α	Acceleration
16^4	6.0	~ 0.1	no	1.8	$(1.5, 0.5)$	0.6	25%
					$(1.0, 1.0)$	0.5	36%
			yes	1.0	$(1.5, 0.5)$	0.5	37%
					$(1.0, 1.0)$	0.4	40%
32^4	6.0	~ 0.1	no	1.8	$(1.5, 0.5)$	0.6	22%
					$(1.0, 1.0)$	0.5	30%
			yes	1.0	$(1.5, 0.5)$	0.4	39%
					$(1.0, 1.0)$	0.4	39%
16^4	5.7	~ 0.2	no	1.8	$(1.5, 0.5)$	0.6	38%
					$(1.0, 1.0)$	0.5	39%
			yes	1.0	$(1.5, 0.5)$	0.5	24%
					$(1.0, 1.0)$	0.5	34%

4 Conclusion and Outlook

In this paper, we examined the effect of the improved form of the domain-wall fermion operator on the convergence of the linear equation solver. The results are summarized in Table 1 for $m = 0.001$ and $L_s = 8$. In a wide range of parameters, the modified form indeed improves the convergence of the even-odd preconditioned CG solver about several tens percent, in the range of 20–40% for our smallest value of the quark mass that requires iterations until convergence most. The required modification of the simulation code is small and the increase in the arithmetic operations is negligible compared to the observed gain. Indeed, in a modern simulation environment where the memory bandwidth or communication overhead is more relevant to the performance than the arithmetic operations, this modification has little effect on the simulation time. Thus the practical use of the improved form of domain-wall fermion matrix is highly attractive.

In a future release, the Bridge++ code set will incorporate the improved form as the standard implementation of the domain-wall fermion matrix.

Acknowledgment. We thank the members of the Bridge++ project, Tatsumi Aoyama, Kazuyuki Kanaya, Yusuke Namekawa, Hidekatsu Nemura, and Keigo Nitadori, for useful discussions. The code development and measurement were performed on the Cygnus and Pegasus systems at University of Tsukuba and Wisteria/BDEC-01 at University of Tokyo through the Multidisciplinary Cooperative Research Program in Center for Computational Sciences, University of Tsukuba. The code development was also done on the Supercomputer Fugaku (through Usability Research ra000001) at RIKEN Center for Computational Science. This work is supported by JSPS KAKENHI (JP20K03961, JP22H00138, JP23K22495), MEXT as "Program for Promoting Researches on the Supercomputer Fugaku" (Simulation for basic science: approaching the new quantum era, PMXP1020230411) and Joint Institute for Computational Fundamental Science (JICFuS).

References

1. Akahoshi, Y., et al.: General purpose lattice QCD code set Bridge++ 2.0 for high performance computing. J. Phys. Conf. Ser. **2207**(1), 012053 (2022). https://doi.org/10.1088/1742-6596/2207/1/012053
2. Arthur, R., et al.: Domain Wall QCD with Near-Physical Pions. Phys. Rev. D **87**, 094514 (2013). https://doi.org/10.1103/PhysRevD.87.094514
3. Borici, A.: Truncated overlap fermions: the link between overlap and domain wall fermions. NATO Sci. Ser. C **553**, 41–52 (2000)
4. Bridge++ project: Lattice QCD code Bridge++. https://bridge.kek.jp/Lattice-code/ (2012)
5. Brower, R.C., Neff, H., Orginos, K.: The Möbius domain wall fermion algorithm. Comput. Phys. Commun. **220**, 1–19 (2017). https://doi.org/10.1016/j.cpc.2017.01.024
6. Brower, R.C., Neff, H., Orginos, K.: Mobius fermions: improved domain wall chiral fermions. Nucl. Phys. B, Proc. Suppl. **140**, 686–688 (2005). https://doi.org/10.1016/j.nuclphysbps.2004.11.180

7. Chen, W.L., Kanamori, I., Matsufuru, H.: Lattice QCD code on GPUs: implementation and performancecomparison with OpenACC and CUDA. In: Proceedings of the International Conference on High Performance Computing in Asia-Pacific Region, pp. 80–89. HPCASIA '25, Association for Computing Machinery, New York, NY, USA (2025). https://doi.org/10.1145/3712031.3712327
8. Chiu, T.W.: Optimal domain wall fermions. Phys. Rev. Lett. **90**, 071601 (2003). https://doi.org/10.1103/PhysRevLett.90.071601
9. Colquhoun, B., Hashimoto, S., Kaneko, T., Koponen, J.: Form factors of $B \to \pi \ell \nu$ and a determination of —VUB— with Möbius domain-wall fermions. Phys. Rev. D **106**(5), 054502 (2022). https://doi.org/10.1103/PhysRevD.106.054502
10. Furman, V., Shamir, Y.: Axial symmetries in lattice QCD with Kaplan Fermions. Nucl. Phys. B **439**, 54–78 (1995). https://doi.org/10.1016/0550-3213(95)00031-M
11. Ginsparg, P.H., Wilson, K.G.: A Remnant of chiral symmetry on the lattice. Phys. Rev. D **25**, 2649 (1982). https://doi.org/10.1103/PhysRevD.25.2649
12. Hasenfratz, P., Laliena, V., Niedermayer, F.: The Index theorem in QCD with a finite cutoff. Phys. Lett. B **427**, 125–131 (1998). https://doi.org/10.1016/S0370-2693(98)00315-3
13. Kaplan, D.B.: A Method for simulating chiral fermions on the lattice. Phys. Lett. B **288**, 342–347 (1992). https://doi.org/10.1016/0370-2693(92)91112-M
14. Luscher, M.: Exact chiral symmetry on the lattice and the Ginsparg-Wilson relation. Phys. Lett. B **428**, 342–345 (1998). https://doi.org/10.1016/S0370-2693(98)00423-7
15. Morningstar, C., Peardon, M.J.: Analytic smearing of SU(3) link variables in lattice QCD. Phys. Rev. D **69**, 054501 (2004). https://doi.org/10.1103/PhysRevD.69.054501
16. Neff, H.: A better conditioned Domain Wall Operator (2015). 1501.04950 [hep-lat]
17. Shamir, Y.: Chiral fermions from lattice boundaries. Nucl. Phys. B **406**, 90–106 (1993). https://doi.org/10.1016/0550-3213(93)90162-I